Interplay of zero-field splitting and excited state geometry relaxation in *fac*-Ir(ppy)$_3$

J. P. Gonzalez-Vazquez[1], P. L. Burn[†2] and B. J. Powell*[1]

[1]Centre for Organic Photonics & Electronics, School of Mathematics and Physics, The University of Queensland, QLD 4072, Australia

[2]Centre for Organic Photonics & Electronics, School of Chemistry and Molecular Biosciences, The University of Queensland, QLD 4072, Australia

[†] p.burn2@uq.edu.au
* bjpowell@gmail.com

Abstract

The lowest energy triplet state, T_1, of organometallic complexes based on iridium(III) is of fundamental interest, as the behaviour of molecules in this state determines the suitability of the complex for use in many applications, e.g., organic light-emitting diodes. Previous characterisation of T_1 in $Ir(ppy)_3$ suggests that the trigonal symmetry of the complex is weakly broken in the excited state. Here we report relativistic time dependent density functional calculations of the zero-field splitting (ZFS) of $Ir(ppy)_3$ in the ground state (S_0) and lowest energy triplet (T_1) geometries and at intermediate geometries. We show that the energy scale of the geometry relaxation in the T_1 state is large compared to the ZFS. Thus, the natural analysis of the ZFS and the radiative decay rates, based on the assumption that the structural distortion is a small perturbation, fails dramatically. In contrast, our calculations of these quantities are in good agreement with experiment.

Introduction

Phosphorescent organometallic complexes, particularly iridium(III) [Ir(III)] complexes, have enormous potential for use as the active components in applications including photocatalysis[1], biological imaging[2], chemical and biological sensing[1], photodynamic therapy[1], light-emitting electrochemical cells[3,4] and organic light-emitting diodes (OLEDs)[5-7]. A key process in such complexes is that excited states quickly relax (non-radiatively) to the lowest energy triplet excitation, T_1. As this occurs on a timescale that is extremely fast compared to the radiative and non-radiative decay rates[5-8], the suitability of a complex for a particular application is determined by the properties T_1. Therefore, in order to understand current materials, and design new complexes, a detailed understanding of T_1 is vital[7,9]. By definition a triplet state consists of three substates and, e.g., relativistic effects can cause these substates to have quite different properties. Therefore a full understanding of T_1 requires, for example, an explanation of the radiative and non-radiative decay rates associated with the three substates and their relative energies, i.e., the zero-field splitting (ZFS) of T_1.

Spin-orbit coupling (SOC) plays a crucial role in at least two of the processes described above. Firstly, the funnelling of singlet excitations into T_1 requires fast inter-system crossing, which can only occur if there is strong SOC. Secondly, phosphorescence is spin-forbidden so SOC is required to allow emission from 'triplet' states. SOC is fundamentally a relativistic effect[7,10] and an accurate description of Ir(III) complexes must also include the larger scalar relativistic effects[7,10], such as the enhancement of the mass of electrons traveling at high velocities near the nucleus.

Therefore phosphorescent organometallic complexes represent a challenging problem for first principles approaches, requiring accurate calculation of both the relativistic effects (including SOC) and the ligand field in fairly large systems. Nevertheless, several recent calculations have suggested that time dependent density functional theory (TDDFT) is capable of achieving the required accuracy if both scalar relativistic effects and SOC are adequately treated[7,11-15].

In order to design the next generation of phosphorescent materials for OLED applications it is vital to develop a detailed understanding of the best performing of the current materials. Extremely high external quantum efficiencies have been demonstrated in OLEDs based on Ir(III) complexes, with the green phosphor *fac*-tris(2-phenylpyridyl)iridium(III) [Ir(ppy)$_3$; Fig. 1] a typical exemplar[6,16]. Therefore, there has been considerable interest in experimentally[6,17], computationally[11,12,15] and theoretically[9] characterising the nature of the T_1 emissive state of iridium(III) complexes such as Ir(ppy)$_3$. However, as we will explore below, previous work has not resulted in a consistent picture of the properties of the three substates of T_1 in Ir(ppy)$_3$ let alone the multitude of complexes that have reported – some of which are highly efficient and others not. In this work we use *fac*-Ir(ppy)$_3$ as a workhorse model as there is sufficient experimental evidence to enable comparison with theory.

Because of the complexity of describing the substates of T_1 from first principles it is often helpful to describe the substates of a triplet level via the so-called "spin Hamiltonian"[7,18]:

$$H = D_s\left(S_z^2 - \frac{2}{3}\right) + E_s\left(S_x^2 - S_y^2\right), \qquad (1)$$

where D_s and E_s parameterise the trigonal and rhombic terms in the fine structure respectively, S_x, S_y and S_z are the Cartesian components of electronic spin operator, and the *z*-axis is taken to be parallel to the C_3 symmetry axis of the complex. In this parameterisation, the $T_z = \frac{1}{\sqrt{2}}(\alpha\beta + \beta\alpha)$ state has energy $-\frac{2}{3}D_s$ and the $T_y = \frac{-i}{\sqrt{2}}(\beta\beta + \alpha\alpha)$ and $T_x = \frac{1}{\sqrt{2}}(\beta\beta - \alpha\alpha)$ have energies $\frac{1}{3}D_s \pm E_s$.

The measured structure of the *fac*-Ir(ppy)$_3$ is C_3 symmetric[19]. In terms of the spin Hamiltonian[18] this implies that $E_S = 0$. Therefore, in the absence of an external magnetic field, one expects that SOC will split T_1 into a non-degenerate A substate (corresponding to the T_z state in the spin Hamiltonian) and a degenerate pair of E substates (the T_x and T_y states). However, it has been proposed that the excited state is localised to a single ligand[5,9,11,12,17]. If the excited state is localised there will be a subtle lowering of the symmetry and the degeneracy of the E-substates will be lifted – resulting in three distinct substates of T_1, which we henceforth number I-III from lowest (I) to highest (III) energy (most to least stable). The measured[5,17] excitation and emission spectra of *fac*-Ir(ppy)$_3$ reveal three distinct substates of T_1 and that the energy difference between states I and II, $\Delta_{I,II}$, is an order of magnitude less than that between state II and III, $\Delta_{II,III}$.

Yersin *et al*.[5,17] have shown that the experimentally determined ZFS is sensitive to the solvent in which the experiment is performed[5,17]: in CH_2Cl_2 $\Delta_{I,II} = 19$ cm^{-1} and $\Delta_{II,III} = 151$ cm^{-1} whereas in poly(methyl methacrylate) (PMMA) $\Delta_{I,II} = 12 - 12.4$ cm^{-1} and $\Delta_{II,III} = 102 - 123$ cm^{-1} and in tetrahydrofuran (THF) $\Delta_{I,II} = 13 - 14$ cm^{-1} and $\Delta_{II,III} = 72 - 136$ cm^{-1}. (The ZFS in CH_2Cl_2 was determined from emission and excitation measurements at 4.2 K and is consistent with the decay rates measured in the temperature range 1.5-300 K; the ZFSs in PMMA and THF were determined from fits to the decay rates in the above temperature range.) Furthermore, Yersin *et al*.[5,17] have shown that magnetic fields up to 12 T do not split any of the levels (I, II or III) but stabilises substate I, destabilises substate II, and leaves the energy of substate III unchanged. This led Yersin *et al.* to assign the states I-III as arising from an ^{3}A excitation in the C_3 molecule with ZFS partially lifting the spin degeneracy of this triplet into an A and E substates and a distortion away from exact C_3 symmetry lifting the degeneracy of the E states. Therefore the natural interpretation of this experiment is that $|D_S| \gg |E_S|$ and $D_S < 0$. This leads to the assignment that state III corresponds to T_z.

However, TDDFT calculations that include SOC[7,11,12,15] are inconsistent with the above assignment [once SOC is included spin is no longer a strict quantum number, but in Ir(ppy)$_3$ SOC is small enough for this label to remain helpful]. For example, calculations[7,12,15] that assume C_3 symmetry find that the A substate is lower in energy than the E substates, i.e, $D_S > 0$. When DFT is used to optimise the geometry with the complex constrained to the T_1 electronic state it is found that the C_3 symmetry is broken and the excitation is localised to a single ligand[7,11,12], cf., also Fig. 2d-g. However, TDDFT calculations have given rather different pictures of the ZFS in the T_1 geometry. Jansson *et al*.[12] worked in the same coordinate frame as us and found that $D_S = 62$ cm^{-1} and $E_S = -8$ cm^{-1} (i.e., $\Delta_{I,II} = 54$ cm^{-1} and $\Delta_{II,III} = 15$ cm^{-1}, with the energies of the substates ordered T_z<T_Y<T_x). Nozaki[11] employed a coordinate system with z-axis bisecting the chelate angle of one ligand and the y-axis in the plan of that ligand and calculated that $D_S = 36$ cm^{-1} and $E_S = -53$ cm^{-1} ($\Delta_{I,II} = 17$ cm^{-1} and $\Delta_{II,III} = 90$ cm^{-1}, with the states ordered T_Y<T_z<T_x; because phase information was not reported it is not possible for us to transform between coordinate frames).

Thus previous TDDFT calculations of the ZFS are inconsistent with one another and experiments, and in particular the sign of D_S and the values of D_S and E_S are questionable. This is a very important problem as it suggests that first principles calculations may not correctly describe the substates of T_1. However, it is interesting to note that these calculations do seem to correctly predict the radiative decay rates in particular it is found that $k_R^I \ll k_R^{II} \ll k_R^{III}$ both experimentally[5,17] and theoretically[11,13,15]. If however the energies of the substates, and in particular their ordering energetically, are incorrect in the TDDFT calculations it suggests that this agreement may be fortuitous.

Methods

Geometry optimisation of the triplet state was performed using the Amsterdam Density Functional (ADF) 2010.01 program[20,21]. The calculation was carried out with the generalized-gradient approximation (GGA) BP86 functional[22] and a TZ2P basis of Slater type orbitals. The ground state geometry with C_3 symmetry enforced is as previously reported[15]. This methodology has been shown previously to accurately reproduce the experimentally observed structures of Ir(III) complexes[7,15,23,24].

TDDFT calculations were carried out with the ADF 2013.01 program[20,21]. One-component zeroth order regular approximation[10] TDDFT calculations, with SOC included perturbatively, were performed on the fifty lowest scalar relativistic singlet and triplet excitations. Including SOC as a perturbation to the scalar zeroth order regular approximation, which gives essentially the same results as those obtained from more expensive two-component methods[14,15], and is more easily related to the underlying molecular orbital excitations.

All TDDFT calculations use a TZP basis and B3LYP functional[25]. Extensive benchmarking calculations have shown that the choice of basis set has a large effect on the calculated energies and that the TZP basis is the minimum required to get good agreement with experiment[15]. Similarly, comparisons of TDDFT calculations using a wide variety of different exchange-correlation functionals with MCD and optical spectra show that B3LYP calculations provide accurate descriptions of the excitation energies observed experimentally[23,24].

Calculations were performed on both the VAYU and RAIJIN clusters at the Australian National Computing Infrastructure National Facility (NCI-NF). The VAYU cluster is comprised of Infiniband connected nodes of Sun X6275 blade servers each containing two quad-core 2.93 GHz Intel CPUs and 24 Gbytes of accessible memory while RAIJIN is a high-performance distributed-memory cluster based on Intel Sandy Bridge 8-core processors (2.6 GHz) with approximately 160 TBytes of main memory.

Results

We carried out all electron scalar relativistic TDDFT calculations *in vacuo* at the optimised T_1 geometry (cf. Table 1) and included SOC perturbatively (see Methods for details). We find that $\Delta_{I,II} = 32$ cm^{-1} and $\Delta_{II,III} = 119$ cm^{-1}, in good agreement with experiment, particularly considering the observed solvent shift. Nevertheless, we find that $D_S = 92$ cm^{-1} and $|E_S| = 59$ cm^{-1}, i.e., state I is predominately T_z, state II is predominately T_y and state III is predominately T_x.

In order to understand why the simple intuition that $|D_S| \gg |E_S|$ fails in both our and previous predictions we have performed calculations using scalar relativistic DFT, scalar relativistic TDDFT and scalar relativistic TDDFT with SOC included perturbatively at a range of geometries that extrapolate linearly between the optimised S_0 and T_1 structures. As we will not focus here on the details of the excited state relaxation mechanism, but rather on how the SOC acts to determine the physical properties of Ir(III) complexes in the T_1 geometry, the exact path followed is not important in these calculations. This linear extrapolation allows a single number to parameterise the geometry, we choose to express this as a percentage with 0 % indicating the S_0 geometry and 100 % corresponding to the T_1 geometry. Thus, for example, in the 50 % geometry all atoms are at the midpoints between their positions in the S_0 and T_1 geometries.

In Fig. 2a we plot the energies of the Kohn-Sham molecular orbitals calculated from scalar relativistic DFT. The changes in the electronic structure are consistent with expectation, i.e., the geometrical changes have a weak perturbative effect on the molecular orbitals, lifting the degeneracies associated with the C_3 symmetry, but do not cause a large shift in the energies.

We plot the lowest energy singlet and triplet excitations calculated from scalar relativistic TDDFT in Fig. 2b,c. Again it can be seen that the degeneracy of the E-symmetry triplets is lifted by the perturbation. However, for the excitations we also see level crossings, which are not observed in the molecular orbitals. This difference is straightforward to understand: the change in geometry causes comparable energy shifts in both the molecular orbitals and the excitations – but the excitations are more densely packed (in energy) than the molecular orbitals; simple combinatorics dictates that there are $2nv$ single excitations for a system of n occupied orbitals and v virtual orbitals.

The underlying cause of the geometry change in the triplet state is made clear by examining the $S_0 \rightarrow T_1$ transition density (i.e., the overlap of the ground and excited state wavefunctions) for various geometries. At the S_0 (0 %) geometry the $S_0 \rightarrow T_1$ transition transforms according to the A representation of C_3. Consistent with this the transition density is evenly distributed across all three ligands. At the T_1 (100 %) geometry the transition is strongly localised to a single ligand and a single Ir-d orbital. This is consistent with a previous analysis of the frontier molecular orbitals in the S_0 and T_1 geometries[7,12] - the $S_0 \rightarrow T_1$ transition is known to be of predominately HOMO→LUMO character[7,15]. We have also examined transition density at intermediate geometries and find that only very small distortions are required to localise the transition. For example in Fig. 2e,f we plot the transition densities at the 2.35 % and 12.5 % geometries – while the former remains delocalised over all three ligands, the latter is already strongly localised.

In order to address the ZFS one needs to describe the effects of SOC, and we do so via second order perturbation theory as this has been shown to accurately reproduce a full relativistic treatment of $Ir(ppy)_3$ and similar Ir(III) complexes[13-15]. In Fig. 3 we plot the energy of the three substates of T_1 as the conformation evolves between the S_0 and T_1 geometries. Surprisingly, even very small distortions cause large relative energy shifts. In particular we only find $\Delta_{I,II} > \Delta_{II,III}$ for geometries very close to the S_0 geometry and hence very close to full C_3 symmetry. For geometries with greater than ~1 % distortion we find $\Delta_{I,II} < \Delta_{II,III}$. Note in particular that we can exclude the possibility that D_s changes sign as the molecule is distorted as this would cause level crossings between the substates of T_1, which are not seen in our calculations.

Thus we have two perturbations to the scalar relativistic calculation in C_3 symmetry: namely the SOC and the C_1 distortion in the T_1 geometry. It is therefore important to ascertain the relative size of these two terms. To understand this in Fig. 4 we compare the ZFS with the reorganisation energy, λ, defined as the energy of the S_0 state at a given geometry relative to the energy at the optimised S_0 geometry. It is immediately clear from these calculations that, in the T_1 geometry, the relaxation energy is large compared to the ZFS – indeed the former is an order of magnitude larger than the latter. However, it is also interesting to ask how the ZFS compares to the relaxation energy at intermediate distortions. There are a number of ways in which one could choose to define this – for example, one could measure the ZFS via $\Delta_{I,II}, \Delta_{II,III}, D_s$ or E_s and one could define the relaxation energy with reference to the change in the energy of the S_0 or the T_1 state. Nevertheless, whatever convention is taken it is clear that a distortion of only a few percent is sufficient to render the reorganisation energy the same order of magnitude as the ZFS. At this point the normal expectation for the ZFS of the T_1 substates, in particular that $|D_s| \gg |E_s|$, breaks down as this is implicitly based on a perturbative treatment of the C_1 distortion.

In contrast, for all of the geometries considered here, the reorganisation energy is smaller than or comparable to the energetic separation of singlet excitations, triplet excitations and molecular orbitals, cf. Fig 2a-c. Indeed for the singlets, triplets and molecular orbitals, the energy to which the degeneracy of the E states is lifted is of order the relaxation energy, which demonstrates that, on these energy scales, the geometry distortion remains a small (linear) perturbation on the larger energy scales that arise in the scalar relativistic calculation.

In the T_1 geometry we find that the radiative rates of the three substates are: $k_R^I = 1.2 \times 10^4\ \mathrm{s}^{-1}$, $k_R^{II} = 8.4 \times 10^4\ \mathrm{s}^{-1}$ and $k_R^{III} = 3.6 \times 10^5\ \mathrm{s}^{-1}$, in reasonable agreement with experimentally measured values (which are $k_R^I = 5.7 \times 10^3\ \mathrm{s}^{-1}$, $k_R^{II} = 5.8 \times 10^4\ \mathrm{s}^{-1}$ and $k_R^{III} = 2.9 \times 10^6\ \mathrm{s}^{-1}$)[5,17]. In Fig. 5 we plot the calculated radiative rates of the three substates for different geometries. The evolution of the radiative rates as the geometry is varied is highly non-trivial and care must be taken in interpreting these results as the linear path followed will presumably not pass through the transition state (saddle point) and therefore the evolution of the radiative rates may be somewhat different from those associated with the true Jahn-Teller distortion[9]. Nevertheless, at small distortions we see a simple linear shift in these rates, consistent with the expectations of perturbation theory in the distortion. However, as the distortion increases we see dramatic changes in the decay rates consistent with the failure of the simple (low order) perturbation theory picture. Most notably at small distortions $k_R^{II} > k_R^{III} > k_R^I$ but for geometries above about 10 % T_1 we find that $k_R^{III} > k_R^{II} > k_R^I$. The change can be understood because the geometry relaxation also drives significant changes in the singlet spectrum – for example, the S_1-T_1 gap decreases by ~10 % between the S_0 and T_1 geometries (cf. Fig. 2b,c). The radiative rates are particularly sensitive to the energy differences between the singlet and triplet states, and different substates mix differently with different singlets. This drives the changes in radiative rate as the geometry relaxes. Furthermore, the oscillator strengths of the singlet states that substates II and III mix most strongly with vary strongly as the geometry is changed. This means that precise determination of the excited state geometry is extremely important if one wants to predict the radiative decay rates of the substates of T_1 with high accuracy.

Finally, we note the large changes we find in both the ZFS and the radiative decay rates with geometry give a natural explanation of the changes observed experimentally in different solvents.[5,17]

Discussion

We have provided a simple explanation for the observation that $\Delta_{II,III} \gg \Delta_{I,II}$ in highly emissive $Ir(ppy)_3$, namely that on the scale of the ZFS the energies associated with the changes in geometry are large. Therefore, the intuition that $|D_s| \gg |E_s|$, which is based implicitly on a perturbative treatment of the geometric relaxation in the T_1 state, is incorrect. Rather we find that $D_s \gtrsim |E_s|$ for even very small distortions away from C_3 symmetry. This further demonstrates that relativistic TDDFT provides a qualitatively and quantitatively accurate description of the substates of T_1 (i.e., the right answer for the right reason), which are the key electronic states involved in the phosphorescence of $Ir(ppy)_3$. Finally, we note that this description is entirely consistent with a recently proposed semi-empirical model of pseudo-octahedral complexes[9]. Together this model and the first principles calculations reported above provide a powerful combination of insight and material specific accuracy.

Knowledge of the emissive dipoles related to T_1 will enable molecular engineering of guest-host combinations that will enable maximum light out-coupling. Thus future application of this approach to related complexes will provide important information for designing highly efficient devices based on complexes with properties tailored for specific applications. Interestingly it has been recently

reported that degradation of iridium(III) complexes can occur by ligand dissociation[26]. Our results show that localisation of the excited state leads to distortion of the complex and it is not unreasonable to consider an extreme distortion as ligand dissociation. Hence, this approach to understanding the optoelectronic properties of iridium(III) complexes has the possibility to provide insight into device stability.

Competing financial interests

The authors declare no competing financial interests.

Acknowledgements

This work was supported by the CSIRO Flagship Collaboration Fund. P.L.B. is supported by a University of Queensland Vice-Chancellor's Senior Research Fellowship. B.J.P. is supported by an Australian Research Council (ARC) Future Fellowship (FT130100161). Calculations we performed on the NCI-NF, which is supported by the ARC under grant LE120100181.

	S_0 geometry (C_3) [Å]	T_1 geometry (C_3) [Å]	Difference (S_0-T_1) [Å]
Ir-C (ppy 1)	2.036	2.038	-0.002
Ir-C (ppy 2)	2.036	1.969	0.067
Ir-C (ppy 3)	2.036	2.050	-0.013
Ir-N (ppy 1)	2.168	2.208	-0.040
Ir-N (ppy 2)	2.168	2.164	0.004
Ir-N (ppy 3)	2.168	2.155	0.012

Table 1. Comparison of the key bond-lengths in the S_0 and T_1 geometries.

Figure 1. The chemical structure of $Ir(ppy)_3$.

Figure 2. Changes in the excitation spectra and transition densities calculated as $Ir(ppy)_3$ moves from the S_0 to the T_1 geometries; calculated from scalar relativistic (TD)DFT. a) Energies of the frontier Kohn-Sham molecular orbitals in the DFT calculations. Note that the HOMO-1 and LUMO+1 are two-fold degenerate at the S_0 geometry (0%). As the structure is linearly extrapolated to the T_1 geometry (100%) these degeneracies are lifted. The small splitting of these orbital energies suggests that the structural distortion is a perturbation to the electronic structure. b,c) Energy of the lowest-energy triplet (b) and singlet (c) excitations from scalar relativistic TDDFT calculations in geometries extrapolating from the S_0 to T_1 geometry – lines are guides to the eye. In both the triplets (b) and singlets (c) one observes the splitting of the twofold degenerate E excited states, as in the molecular orbitals, but also several level crossings, which are not seen in the molecular orbitals. d-g) Transition density (product of initial and final states of an excitation) of the first triplet excited state, T_1, of $Ir(ppy)_3$ at four different geometries.

Figure 3. Energies of the substates of T_1 from relativistic TDDFT calculations as the geometry is varied between the S_0 geometry (0 %) and the T_1 geometry (100 %). At the S_0 geometry, which has C_3 symmetry, the non-degenerate (A) substate is lower in energy than the two-fold degenerate (E) states. The relaxation in the excited state breaks the trigonal symmetry of the complex. Even small distortions rapidly lift the degeneracy of the E states (see inset, which shows the same data over a reduced range to more clearly show the effects of small distortions). Indeed, a ~1 % distortion already causes a large enough splitting of these states to make $\Delta_{I,II} \sim \Delta_{II,III}$.

Figure 4. Comparison of the key energy scales for the T_1 state. Even for small distortions (~1 % see inset, which shows the same data over a reduced range) the reorganisation energy, λ, is comparable to the electronic energy scales that characterise the triplet, $\Delta_{I,II}$, $\Delta_{II,III} = 2E_s$, and D_s. The reorganisation energy in the T_1 geometry (0.30 eV) is an order of magnitude larger than the

electronic energy scales. This means that the geometry relaxation cannot be viewed as a perturbation to the T_1 substates and explains why $D_s \approx E_s$ (or, equivalently why, $\Delta_{I,II} \ll \Delta_{II,III}$).

Figure 5. Radiative decay rates of the three substates of T_1. For small distortions the breaking of C_3 symmetry leads to a simple linear shift in the radiative decay rates, as would be expected from perturbation theory (cf. inset, which shows the same data over a reduced range). However, for larger distortions clear non-linear, indeed non-monotonic, behaviour is observed. This underlines the general finding that the changes to the substates of T_1 when the complex is distorted from the S_0 to T_1 geometries cannot be correctly understood in a simple perturbative framework.

Figure 1

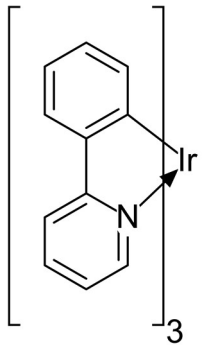

Figure 2

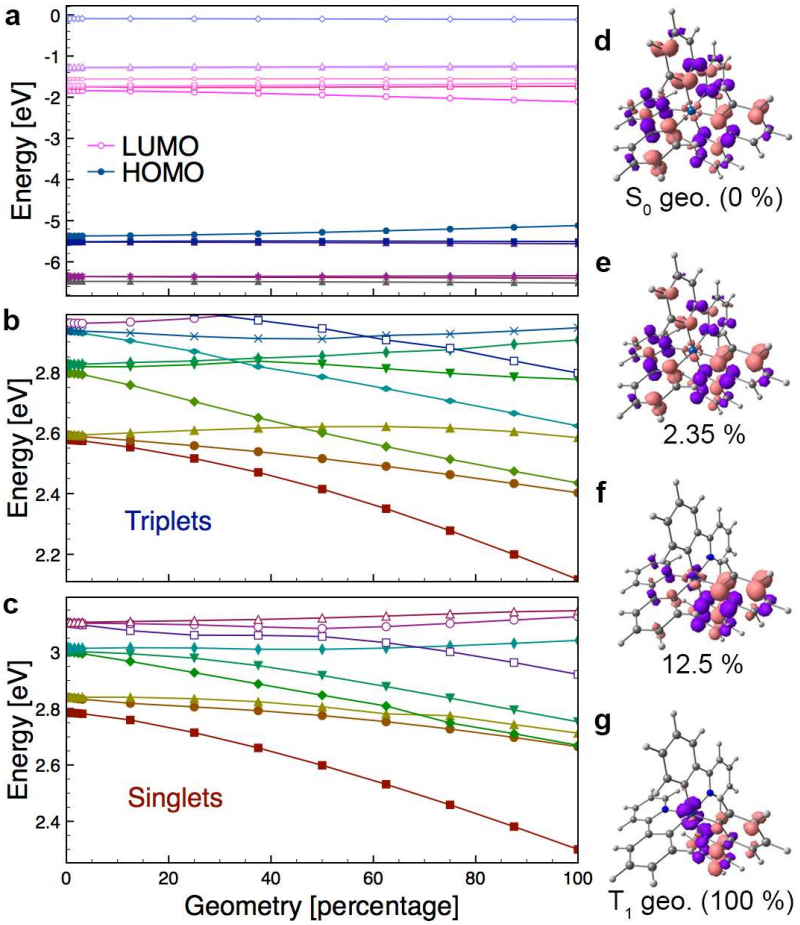

Figure 3

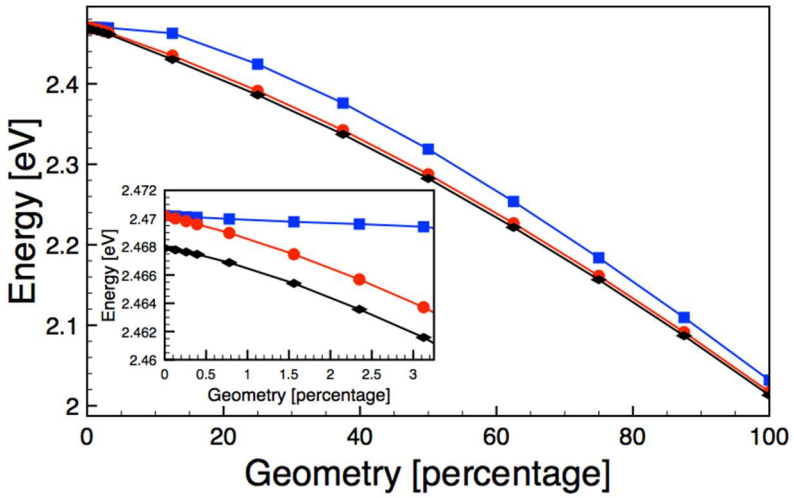

Figure 4

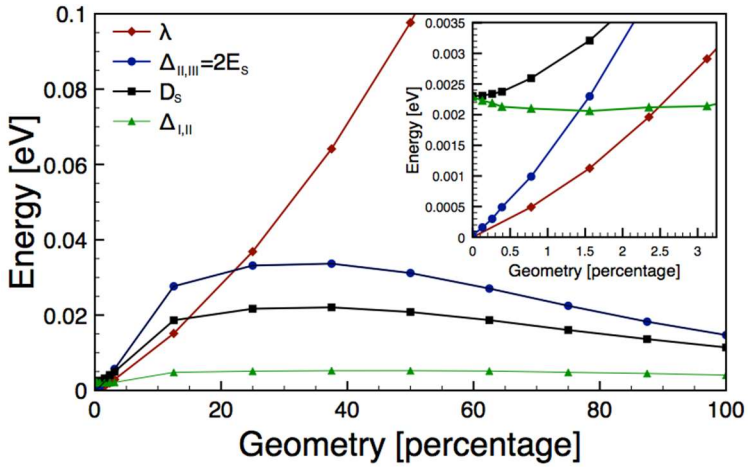

Figure 5

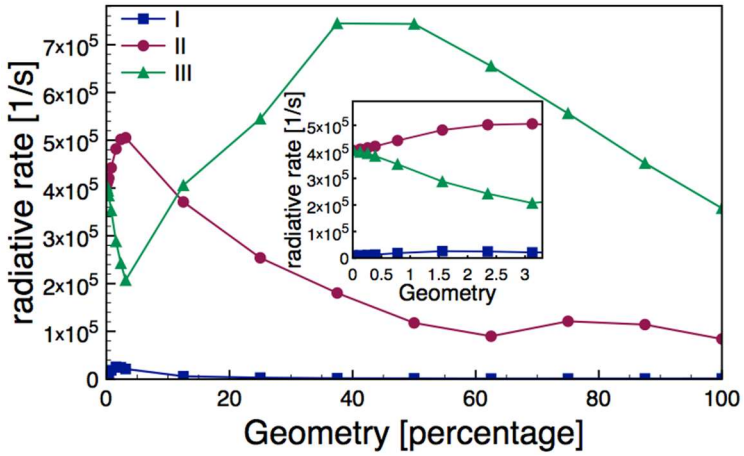

For Table of Contents Only

We report relativistic time dependent density functional calculations of the zero-field splitting (ZFS) of $Ir(ppy)_3$ in the ground state (S_0) and lowest energy triplet (T_1) geometries and at intermediate geometries. The energy scale of the geometry relaxation in the T_1 state is large compared to the ZFS. Thus, the usual analysis, assuming that the structural distortion is a small perturbation, fails dramatically. In contrast, our calculations of these quantities are in good agreement with experiment.

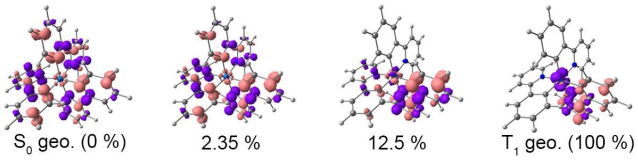

References

(1) You, Y.; Park, S. Y. *Dalton Trans.* **2009**, 1267-1282.

(2) Yu, M.; Zhao, Q.; Shi, L.; Li, F.; Zhou, Z.; Yang, H.; Yi, T.; Huang, C. *Chem. Commun.* **2008**, 2115-2117.

(3) Bolink, H. J.; Coronado, E.; Costa, R. D.; Lardiés, N.; Ortí, E. *Inorg. Chem.* **2008**, *47*, 9149-9151.

(4) Su, H.-C.; Chen, H.-F.; Fang, F.-C.; Liu, C.-C.; Wu, C.-C.; Wong, K.-T.; Liu, Y.-H.; Peng, S.-M. *J. Am. Chem. Soc.* **2008**, *130*, 3413-3419.

(5) Yersin, H.; Rausch, A. F.; Czerwieniec, R.; Hofbeck, T.; Fischer, T. *Coord. Chem. Rev.* **2011**, *255*, 2622-2652.

(6) Yersin, H. *Highly Efficient OLEDs with Phosphorescent Materials*; Wiley: Weinheim, 2008.

(7) Powell, B. J. *Coord. Chem. Rev.* **2015**, *295*, 46–79.

(8) Yoon, S.; Kukura, P.; Stuart, C. M.; Mathies, R. A. *Mol. Phys.* **2006**, *104*, 1275-1282.

(9) Powell, B. J. *Sci. Rep.* **2015**, *5*, 10815.

(10) Dyall, K. G.; Fægri, K. *Introduction to relativistic quantum chemistry*; Oxford University Press: New York, 2007.

(11) Nozaki, K. *J. Chin. Chem. Soc.* **2006**, *53*, 101-112.

(12) Jansson, E.; Minaev, B.; Schrader, S.; Årgen, H. *Chem. Phys.* **2007**, *333*, 157-167.

(13) Jansson, E.; Norman, P.; Minaev, B.; Ågren, H. *J. Chem. Phys.* **2006**, *124*, 114106

(14) Mori, K.; Goumans, T. P. M.; van Lenthe, E.; Wang, F. *Phys. Chem. Chem. Phys.* **2014**, *16*, 14523-14530.

(15) Smith, A. R. G.; Burn, P. L.; Powell, B. J. *ChemPhysChem* **2011**, *12*, 2429-2438.

(16) Baldo, M. A.; Lamansky, S.; Burrows, P. E.; Thompson, M. E.; Forrest, S. R. *Appl. Phys. Lett.* **1999**, *75*, 4-6.

(17) Hofbeck, T.; Yersin, H. *Inorg. Chem.* **2010**, *49*, 9290-9299.

(18) Abragam, A.; Bleaney, B. *Electron paramagnetic resonance of transition ions*; Clarendon Press: Oxford,, 1970.

(19) Berger, R. J. F.; Stammler, H.-G.; Neumann, B.; Mitzel, N. W. *Eur. J. Inorg. Chem.* **2010**, 1613–1617.

(20) te Velde, G.; Bickelhaupt, F. M.; Baerends, E. J.; Guerra, C. F.; van Gisbergen, S. J. A.; Snijders, J. G.; Ziegler, T. *J. Comp. Chem.* **2001**, *22*, 931-967.

(21) Fonseca Guerra, C.; Snijders, J. G.; te Velde, G.; Baerends, E. J. *Theo. Chim. Acta* **1998**, *99*, 391-403.

(22) Becke, A. D. *Phys. Rev. A* **1988**, *38*, 3098-3100.

(23) Smith, A. R. G.; Riley, M. J.; Burn, P. L.; Gentle, I. R.; Lo, S. C.; Powell, B. J. *Inorg. Chem.* **2012**, *51*, 2821-2831.

(24) Smith, A. R. G.; Riley, M. J.; Lo, S.-C.; Burn, P. L.; Gentle, I. R.; Powell, B. J. *Phys. Rev. B* **2011**, *83*, 041105(R).

(25) Becke, A. D. *J. Chem. Phys.* **1993**, *98*, 5648-5652.

(26) Jurow, M. J.; Bossi, A.; Djurovich, P. I.; Thompson, M. E. *Chem. Mater.* **2014**, *26*, 6578-6584.